Volume 1 | Number 1 | Jan 2013 | Pages 1–100

PCCP

Physical Chemistry Chemical Physics
www.rsc.org/pccp

ROYAL SOCIETY OF CHEMISTRY

Two-dimensional proton-detected ^{35}Cl/^{1}H correlation solid-state NMR experiment under fast magic angle sample spinning: Application to pharmaceutical compounds

Manoj Kumar Pandey[1], Hiroshi Kato[2], Yuji Ishii[2], Yusuke Nishiyama*[1,2]

[1]RIKEN CLST-JEOL collaboration center, RIKEN, Yokohama, Kanagawa 230-0045, Japan

[2] JEOL RESONANCE Inc., Musashino, Akishima, Tokyo 196-8558, Japan

Key words: solid-state NMR; proton-detected; fast MAS; ^{35}Cl; quadrupolar coupling, molecular structure;

*Corresponding author

E-mail address: yunishiy@jeol.co.jp

Tel: +81-42-542-2236

Fax: +81-42-544-1955

Abstract

The determination of structure of hydrochloride salts of active pharmaceutical ingredients (HCl APIs) utilizing ^{35}Cl solid-state NMR studies has been of considerable interest in the recent past. Until now these studies relied on the ^{35}Cl direct observation method which has its own limitations in terms of the sensitivity and resolution due to the quadrupolar nature and low gyromagnetic ratio of ^{35}Cl. In this contribution we successfully demonstrate the measurement of 2D ^{35}Cl/^{1}H correlation experiment by using the proton detection-based (indirect observation of ^{35}Cl via ^{1}H) approach at fast magic angle sample spinning (MAS: 70 kHz). The main advantages of this approach over direct observation method are highlighted in the present study. We have employed heteronuclear magnetization transfer through the recoupling of ^{35}Cl-^{1}H heteronuclear dipolar interactions. The applicability of the ^{35}Cl indirect detection method is first demonstrated on hydrochloride salts of amino acids, L-Tyrosine.HCl and L-Histidine.HCl.H$_2$O following which the 2D ^{35}Cl/^{1}H correlations are obtained for HCl APIs, Procainamide HCl (Proc) and Aminoguanidine HCl (Amin). On the basis of separation between the central transition (CT) and satellite transition (ST) peaks and the shape/width of CT powder pattern, it is also shown that the quadrupolar parameters which are useful for the elucidation of molecular structure can be determined. Moreover, the ^{35}Cl/^{1}H correlations provide the precise determination of ^{1}H chemical shifts of nearby ^{35}Cl nuclei.

Introduction

Hydrochloride salts of active pharmaceutical ingredients (HCl APIs) are known to be present in almost 50% of solid pharmaceuticals available in the market. The role of HCl in such compounds is to increase/control stability, solubility, bioactivity and bioavailability. These compounds exhibit interesting structural features such as polymorphism and pseudo polymorphism, and each polymorph has unique properties towards biochemical activities.[1-4] Subsequently, their structural characterization is always of important consequence in the pharmaceutical industries. In general, single crystal or powder X-ray diffraction (XRD) techniques are used for structural studies of these systems.[5] However, there are always certain limitations associated with these techniques such as difficulty in getting good quality single crystals, and complexity associated with the interpretation of powder XRD data to get detailed information about the polymorphs.[6,7] Furthermore, powder XRD method requires single component sample with a very high purity and as a result it fails when implemented on samples comprising several components. This limits its application in the pharmaceutical industry. Additionally, XRD method has an inherent limitation towards the structural characterization of amorphous solids. As an alternative to XRD, solid-state NMR is recognized as one of the most valuable techniques to get atomic-level insights into the structure and dynamics of pharmaceutical compounds. Since HCl APIs are present in almost 50% of the solid pharmaceuticals sold in the market, ^{35}Cl ($I = 3/2$, quadrupolar moment (Q) = 0.082 x 10^{-28} m^2, and natural abundance: 75.53%) becomes an obvious nucleus of choice for structural characterization using solid-state NMR.[8,9] Although ^{35}Cl nuclei have high natural abundance, their solid-state NMR studies have always been challenging due to low gyromagnetic ratio (γ) and the ringing effect from the probe that dominates the spectrum in the presence of large quadrupolar interactions resulting from a quick decay of FID. Fortunately, NMR-allowed

central transition (CT: -1/2 ↔ +1/2) in the case of half integer nuclei are devoid of any first-order broadening. Nevertheless, powder lineshapes suffer strongly from the second-order quadrupolar broadening ranging from few kHz to several MHz. Although magic angle spinning (MAS) partially reduces the CT line width by getting rid of the second-rank spatial interaction terms from the second-order interaction Hamiltonian, the fourth-rank spatial interactions still remain partially unaveraged. On the basis of spatial and/or spin manipulations, techniques like DOuble Rotation (DOR),[10,11] Dynamic Angle Spinning (DAS)[12] and Multi-Quantum MAS (MQMAS)[13] are known to be effective for the removal of second-order quadrupolar broadening. However, poor sensitivity of low γ nuclei has always been a challenge to overcome using these methods. Although the spectral resolution and sensitivity have been major limitations of solid-state NMR technique, recent advancements in the NMR probe design, which allow magic angle spinning (MAS) up to 120 kHz in combination with the proton detection-based methods, have contributed significantly in overcoming these limitations.[14,15] Specifically, proton detection-based methods for heteronuclear and homonuclear correlations at fast MAS are routinely employed for the indirect observation of quadrupolar nuclei such as ^{14}N ($I = 1$).[16-24] Encouraged with the success of proton-detected experiments involving ^{14}N, we demonstrate the indirect observation of ^{35}Cl in HCl APIs (Procainamide HCl and Aminoguanidine HCl) utilizing the standard D-HMQC pulse sequence at 70 kHz MAS. Subsequently, this method allows us to determine ^{35}Cl quadrupolar/isotropicshift parameters as well as ^{1}H chemical shifts which are quite useful for the molecular structure elucidation. The many advantages of using the proton detection-based method for the study of such systems at fast MAS include 1) improved sensitivity, 2) improved resolution due to the addition of the ^{1}H dimension, 3) well-correlated ^{35}Cl/^{1}H resonances, 4) removal of probe ringing issues, 5) requirement of a small sample

volume, 6) distinction between through bond (J) and space (D) couplings, 7) observation of weak ST if ^{35}Cl is irradiated using a hard pulse with rotor-synchronized acquisition, and 8) short repetition time provided ^{1}H T_1 relaxation time is shorter than ^{35}Cl T_1.

Experimental

Solid-state NMR measurements were carried out either using 700 MHz (JNM-ECA700II, JEOL RESONANCE Inc.) or 600 MHz (JNM-ECZ600R, JEOL RESONANCE Inc.) NMR spectrometers equipped with 1.0 mm triple resonance and double resonance ultrafast MAS probes (JEOL RESONANCE Inc.), respectively. Approximately, 1.0 mg each of L-Tyrosine.HCl, L-Histidine.HCl.H$_2$O, Procainamide HCl (Proc) and Aminoguanidine HCl (Amin) were packed separately into 1.0 mm zirconia rotors and all the experiments were performed at 70 kHz MAS. The pulse sequence implemented to record the 2D ^{35}Cl/^{1}H chemical shift correlations is shown in the Supporting Information (**Figure S1**). 16 dummy scans were applied prior to the start of all the 2D measurements, and the recycle delays were set to 2s, 8s, 120s and 2s for L-Tyrosine.HCl, L-Histidine.HCl.H$_2$O, Amin and Proc, respectively. The proton 90° pulse durations were set to 1.3 and 1.0 μs at 700 and 600 MHz spectrometers, respectively. To maximize the ^{35}Cl-^{1}H magnetization transfer efficiency in the 2D ^{35}Cl/^{1}H correlation experiments ^{35}Cl pulse duration, and both excitation and reconversion periods were optimized carefully. The ^{35}Cl pulse durations were set at 13.5, 13.5, and 8 μs with ~10 kHz (at 700 MHz), 14 and 24 kHz (at 600 MHz) RF field strengths (measured using NH$_4$Cl) for L-Tyrosine.HCl, Amin and Proc, respectively, while SR4 recoupling of duration 0.171 ms was used during the excitation and reconversion periods. The ^{35}Cl pulse duration of 1.35 μs was used in the case of 2D and 1D experiments carried out with hard pulse irradiation on ^{35}Cl for L-Tyrosine.HCl and L-Histidine.HCl.H$_2$O. For the 2D data collection, 32, 32, 16 and 32 increments were set in the t_1

dimension and 640 (for soft pulse ^{35}Cl irradiation) and 768 (for hard pulse ^{35}Cl irradiation), 448, 32 and 1792 scans were collected every t_1 increment for L-Tyrosine.HCl, L-Histidine.HCl.H$_2$O, Amin and Proc, respectively. To achieve pure absorption peaks States-TPPI method was applied in the t_1 dimension. ^{35}Cl isotropic shifts were referenced with respect to ^{35}Cl peak (0 ppm) of solid NH$_4$Cl. All NMR data were processed using Delta NMR software (JEOL RESONANCE Inc.). The ^{1}H 1D projections corresponding to all the 2D ^{35}Cl/^{1}H correlation spectra were obtained by the partial projection of the displayed 2D spectral regions.

Results and Discussion

It is well known that the magnetization transfer in the *J*-HMQC experiment for solids is achieved through bond/scalar coupling (*J*) along with residual dipolar splitting (RDS) resulting from the second-order cross-terms between the quadrupolar and dipolar interactions unlike solution NMR method.[16-21] Consequently, this sequence works best for the samples wherein there is a direct bond between the proton and the heteronucleus. However, *J*-HMQC spectra might suffer from a huge loss in the sensitivity due to ^{1}H transverse relaxation (T_2'), if performed in the systems such as the ones used in the present study with the lack of such chemical bonds as the mode of the magnetization transfer now is mostly through RDS. In an alternate approach known as the D-HMQC experiment,[22-24] sensitivity enhancement in the ^{35}Cl dimension can be obtained from the enhanced magnetization transfer via recoupled large ^{35}Cl-^{1}H heteronuclear dipolar interactions instead of small *J*-coupling and RDS and elongated T_2' by decoupled ^{1}H-^{1}H dipolar interactions. Herein, both excitation and reconversion durations are reduced as a consequence signal decay due to T_2' component is minimized. Moreover, the dwell time of the indirect dimension in the D-HMQC experiment should be synchronized with respect to the sample spinning. The role of fast MAS in such experiments is to 1) provide a wider spectral width required to observe nuclei with

large second-order quadrupolar couplings, 2) increase ^1H T_2' relaxation times due to better suppression of ^1H-^1H homonuclear dipolar interactions such that data can be collected without the need of ^1H-^1H homonuclear decoupling during the t_2 acquisition, and 3) improve efficiency of heteronuclear decoupling during the t_1 evolution.

To test the applicability of proton-detected D-HMQC sequence to get $^{35}Cl/^1H$ correlations in HCl APIs, Amin and Proc, first we carried out the 2D $^{35}Cl/^1H$ correlation experiment on L-Tyrosine.HCl and L-Histidine.HCl.H$_2$O. These were selected as test samples because of their small molecular size, shorter ^1H longitudinal relaxation time (T_1), longer ^1H transverse relaxation time (T_2'), and relatively smaller ^{35}Cl quadrupolar coupling. The proton-detected $^{35}Cl/^1H$ correlation spectrum of L-Tyrosine.HCl collected at 700 MHz spectrometer under 70 kHz MAS using a soft pulse irradiation on ^{35}Cl is shown in **Figure 1B**. The ^{35}Cl shift observed from this experiment was cross validated from the 1D spectrum collected through the direct observation of ^{35}Cl using a single hard pulse experiment. The observed ^{35}Cl experimental along with the simulated powder lineshapes of L-Tyrosine.HCl are shown in **Figure 1A**. As seen from **Figure 1A** the experimental spectrum fits extremely well with the simulated powder lineshape. Additionally, the calculated quadrupolar parameters for L-Tyrosine.HCl (Qcc = 2.3 MHz and η = 0.7), where η is the asymmetry parameter, are found to be in an excellent agreement with the values reported in the literature.[25] The number of $^{35}Cl/^1H$ cross-peaks observed from the proton-detected 2D HMQC experiment (**Figure 1B**) correlates well with the three short ^{35}Cl---^1H contacts (H2-Cl: 2.078 Å, (H1/H5/H9)-Cl: 2.378/2.471/2.505 Å and H3-Cl 2.66 Å) seen from the crystal structure of L-Tyrosine.HCl (Refer to Figure S2 of the Supporting Information).[26,27] Moreover, a longer range $^{35}Cl/^1H$ correlation peak (H6-Cl: 3.874 Å) with a very weak intensity is also seen in the 2D $^{35}Cl/^1H$ correlation spectrum. It is to be noted that ^{35}Cl /^1H correlation spectra

should be recorded with short and longer recoupling times for a clear distinction between short

and longer range ^{35}Cl /^{1}H proximities, respectively, as previously demonstrated by Brown et.al

through ^{14}N-^{1}H correlations in supramolecular and pharmaceutical systems.[28-30] Spectral slices at

^{1}H chemical shifts of 10, 7.7 and 4.5 ppm (parallel to the ^{35}Cl dimension) of the proton-detected

2D ^{35}Cl/^{1}H correlation spectrum (**Figure 1C**) show slightly dissimilar quadrupolar lineshapes.

Since the asymmetric unit cell of L-Tyrosine.HCl has a single ^{35}Cl site,[27] therefore in principle it

should result in identical ^{35}Cl quadrupolar lineshapes at the three ^{1}H resonances. The fact that we

observe dissimilar lineshapes should be attributed to the imperfect ^{35}Cl/^{1}H magnetization transfer

(all crystallites are not excited/transferred uniformly) that more likely depends on the relative

orientation between ^{35}Cl-^{1}H dipolar and ^{35}Cl quadrupolar tensors.[19,31]

Furthermore, the ^{1}H 1D spectral slice (**Figure 2**) at the ^{35}Cl peak position (parallel to the ^{1}H

chemical shift dimension) of the 2D ^{35}Cl/^{1}H correlation spectrum can also be utilized to assign

exact proton resonances that are correlated to ^{35}Cl. As seen from the 1D ^{1}H MAS (**Figure 2**)

spectrum of L-Tyrosine.HCl, two C_β proton resonances (H3/H4) cannot be distinguished due to

severe overlap. On the basis of its crystal structure,[26,27] ^{35}Cl is found to be in a close proximity

(2.66 Å) with only one of the C_β protons (H3) whereas other proton (H4) is located at a longer

distance (3.107 Å). Consequently, the 1D spectral slice from the 2D HMQC spectrum (HMQC

filtered ^{1}H spectrum) results in the signal originating from H3 and not H4 (**Figure 2**). Similarly,

NH resonances (H1/H5/H9) can be distinguished with respect to aromatic proton H7 (5.76 Å)

resonance from the 1D HMQC filtered spectrum. More interestingly, the 1D spectral slice from

the 2D HMQC spectrum (**Figure 2**) results in a weak peak for the carboxyl group proton (H6)

even if it is located at a much longer distance (3.874 Å) from ^{35}Cl in comparison to those protons

that are not observed in the HMQC filtered ^{1}H spectrum. Since this proton is involved in the

protonation of the carboxyl group, therefore it should be regarded as a labile proton with a shorter $^{35}Cl/^{1}H$ distance.

As discussed above, the proton-detected 2D $^{35}Cl/^{1}H$ D-HMQC correlation experiment with a soft pulse irradiation of ^{35}Cl is only capable of providing qualitative information about the quadrupolar interaction due to poor sensitivity and resolution. The limited resolution of the ^{35}Cl peaks in $^{35}Cl/^{1}H$ HMQC spectrum is due to the signal decay resulting from ^{1}H T_2 relaxation and residual $^{1}H-^{35}Cl$ dipolar interactions in the t_1 dimension. While both of which are improved at faster MAS rate, resolution enhancement still remains a challenge in the $^{35}Cl/^{1}H$ HMQC experiments. However, the use of a hard pulse irradiation of ^{35}Cl with rotor-synchronized acquisition in the 2D D-HMQC experiment can provide quantitative information about the quadrupolar interaction. As seen from **Figure 3**, the 2D D-HMQC spectrum collected using a hard pulse (1.35 μs) irradiation of ^{35}Cl resulted in very strong ST peaks along with the CT peaks. This observation is a good contrast to the ^{35}Cl direct observation method that results in a much weaker ST even with a hard pulse excitation. A hard pulse excites a wider range of ^{35}Cl frequencies which also includes ST frequencies resulting in a numerous spinning sideband manifold and hence weaker ST intensities from the direct observation ^{35}Cl. On the other hand, the indirect observation with rotor-synchronized acquisition allows us to fold these spinning sidebands onto the ST peak that results in a remarkable improvement in its sensitivity. Subsequently, the proton detection-based methods can also be utilized to observe ST with comparable signal intensity to CT if a quadrupolar nucleus is irradiated with a hard pulse, which in principle should lead to more accurate determination of quadrupolar parameters. To further validate this viewpoint, we carried out numerical simulations a) by varying Qcc with fixed η (**Figure 4A**) and b) by varying η with fixed Qcc (**Figure 4B**) using a single hard pulse ^{35}Cl

9

excitation and rotor-synchronized acquisition. It is clearly evident from **Figure 4A** that with the increase in Qcc for a fixed η (= 0.7), the separation between ST and CT peaks increases. This peak separation is very sensitive to a small change in the Qcc. Similarly, with the increase in η for a fixed Qcc (2.5 MHz), again the ST and CT peak separation increases (**Figure 4B**). Subsequently, on the basis of the observed ST and CT peak separation and CT powder lineshape, determination of quadrupolar parameters (Qcc and η) with improved accuracy is possible by fitting the experimental ^{35}Cl powder lineshape inclusive of both CT and ST obtained from the indirect observation of ^{35}Cl with a hard pulse irradiation and rotor-synchronized acquisition in the 2D D-HMQC experiment. It is important to mention here that in cases where it is difficult to measure the ^{35}Cl 1D spectrum from the direct observation and, consequently, determine the exact position of its shift, the proton-detected 2D correlation experiment with a soft pulse irradiation of ^{35}Cl that only excites CT frequency becomes mandatory to clearly distinguish CT and ST peaks obtained using a hard pulse irradiation of ^{35}Cl. Finally, the spectral slices taken parallel to the ^{35}Cl shift dimension at ^{1}H chemical shifts of 10, 7.7 and 4.5 ppm of the proton-detected ^{35}Cl/^{1}H 2D D-HMQC correlation spectrum obtained using a hard pulse irradiation of ^{35}Cl are simulated to extract quadrupolar parameters (**Figure 5**). On the basis of the ST and CT peak separation and CT lineshape fitting the extracted quadrupolar parameters associated with ^{35}Cl in contact with different protons are listed in **Figure 5** caption. As expected for the single ^{35}Cl site, the quadrupolar parameters obtained from the lineshape fitting result in almost similar values. As discussed above, a slight variation in the ^{35}Cl lineshapes can be ascribed to the non-uniform ^{35}Cl/^{1}H magnetization transfer that depends on the relative orientation of dipolar and the quadrupolar tensors. It is worthwhile to point out that exact powder lineshape of ^{35}Cl CT spectra obtained from the 1D slices of the ^{35}Cl/^{1}H 2D correlation spectrum could not be matched

precisely with the simulated lineshape and can in principle lead to minor discrepancies in the values of quadrupolar parameters reported in the present study. To achieve a perfect powder lineshape we believe that the proton-detected 2D D-HMQC spectrum should be collected with a larger number of points in the indirect dimension that requires a long experimental time. Moreover, the $^{35}Cl/^{1}H$ 2D correlation experiment performed at faster MAS (> 70 kHz) should also further improve the resolution and sensitivity of powder lineshape.
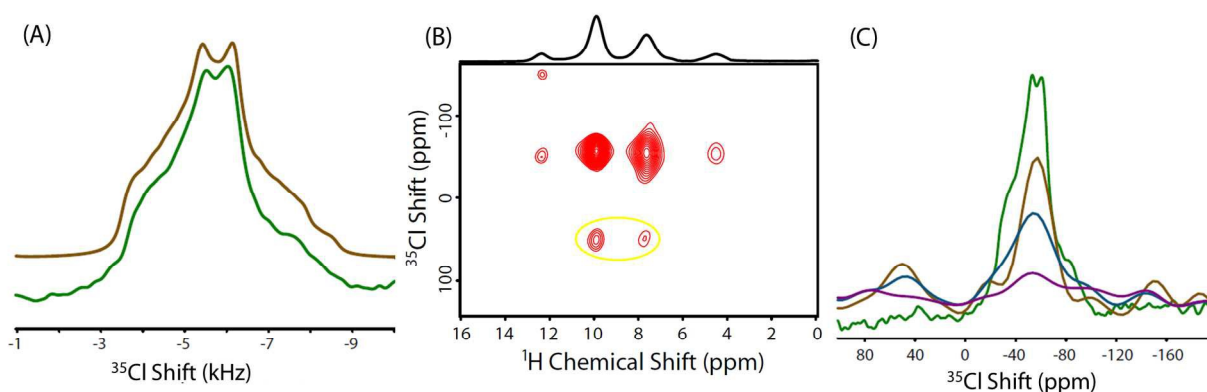

Figure 1. One-dimensional ^{35}Cl experimental (green) spectrum collected using a hard pulse (1.35 μs) excitation and 10,000 scans (total experimental time = 5.6 hours), and simulated lineshape (brown) of L-Tyrosine.HCl (A), a representative 2D $^{35}Cl/^{1}H$ D-HMQC spectrum measured using a soft pulse irradiation on ^{35}Cl (total experimental time = 22.8 hours) (B) and spectral slices at 10 (brown), 7.7 (blue) and 4.5 (magenta) ppm parallel to the ^{35}Cl shift dimension and overlaid with the 1D ^{35}Cl spectrum in green (C). All NMR spectra were collected on 700 MHz spectrometer at 70 kHz MAS. Circled cross-peaks with weaker intensities in (B) are the STs.
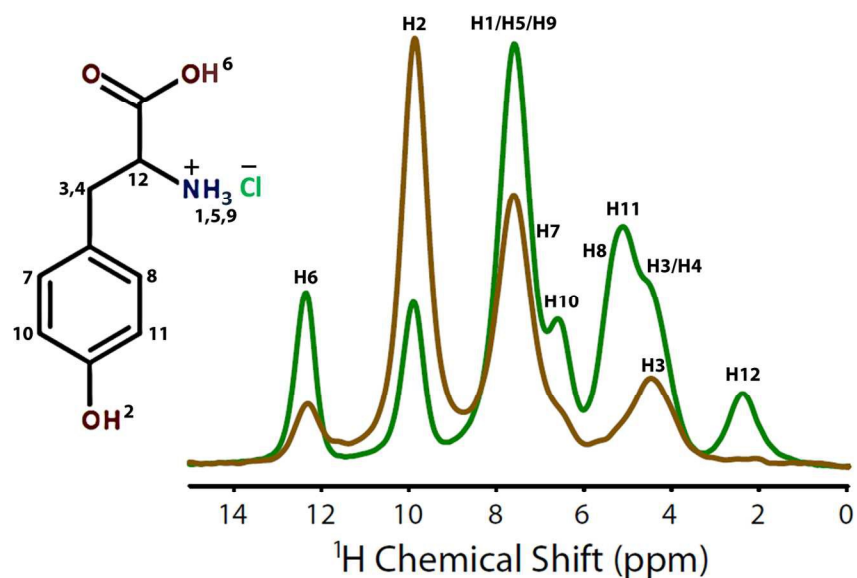
Figure 2. Molecular structure and the 1D ^{1}H MAS spectrum (green) collected using a spin-echo pulse sequence at 70 kHz MAS, and the 1D spectral slice (brown) at the ^{35}Cl peak position from the 2D D-HMQC spectrum of L-Tyrosine.HCl. The proton resonances that are not correlated to ^{35}Cl do not appear in the 1D spectral slice or the HMQC filtered spectrum.
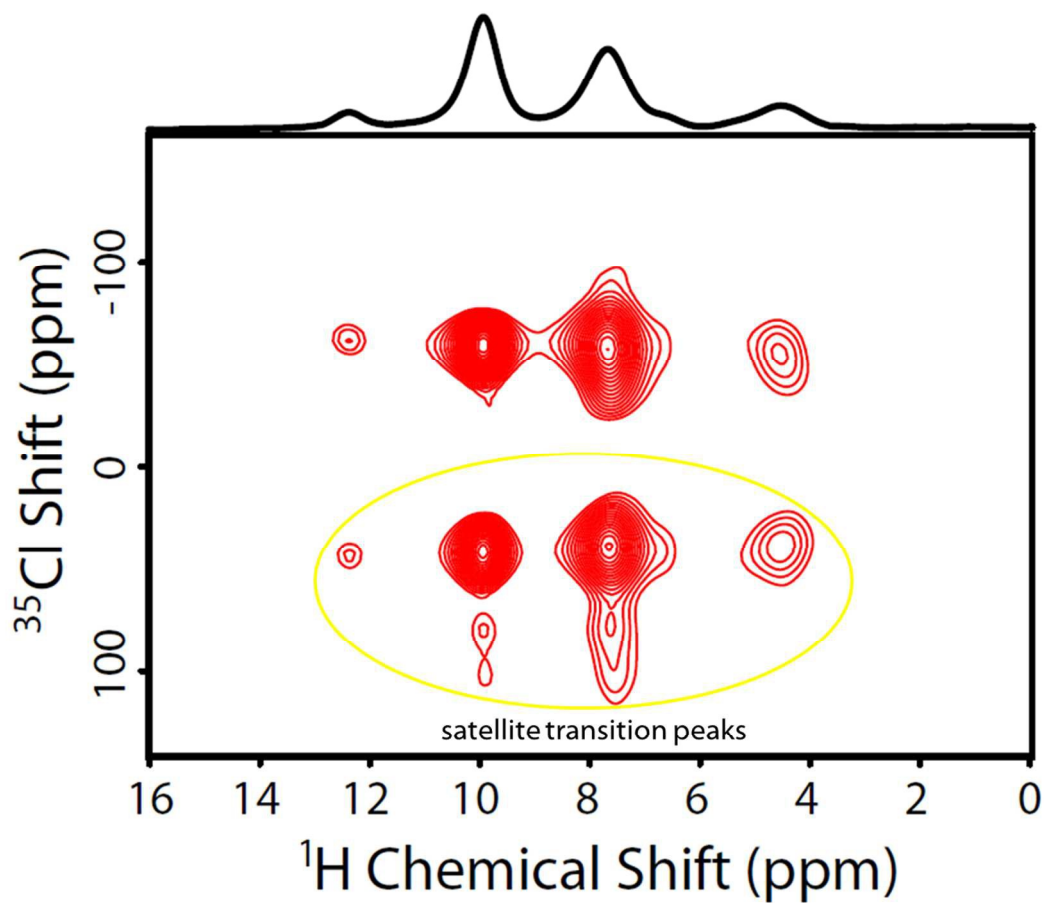
Figure 3: A representative 2D ^{35}Cl/^{1}H D-HMQC spectrum of L-Tyrosine.HCl using a hard pulse (1.35 μs) irradiation on ^{35}Cl (total experimental time = 27.3 hours). Cross-peaks that are circled represent the STs.
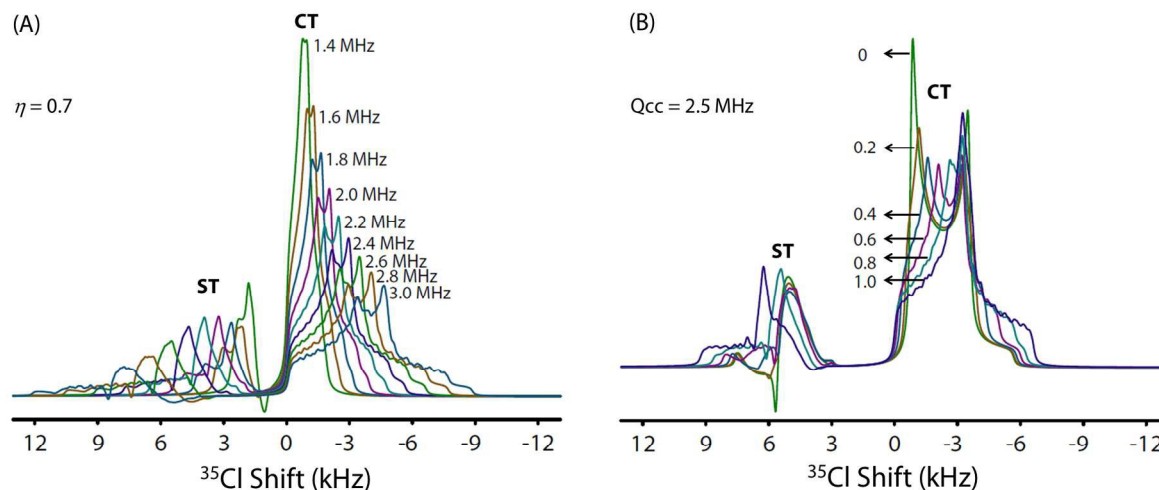
**Figure 4**. Simulated ^{35}Cl 1D quadrupolar lineshapes obtained using a single hard pulse (1.6 µs and RF field = 10 kHz) irradiation by (A) varying Qcc with a fixed η (0.7), and (B) varying η with a fixed Qcc (2.5 MHz). All the 1D simulations were performed under 70 kHz MAS at 700 MHz ^{1}H Larmor frequency with 4180 (α, β) orientations for powder averaging. For the sake of simplicity ^{35}Cl chemical shift parameters were set to zero in all the simulations.
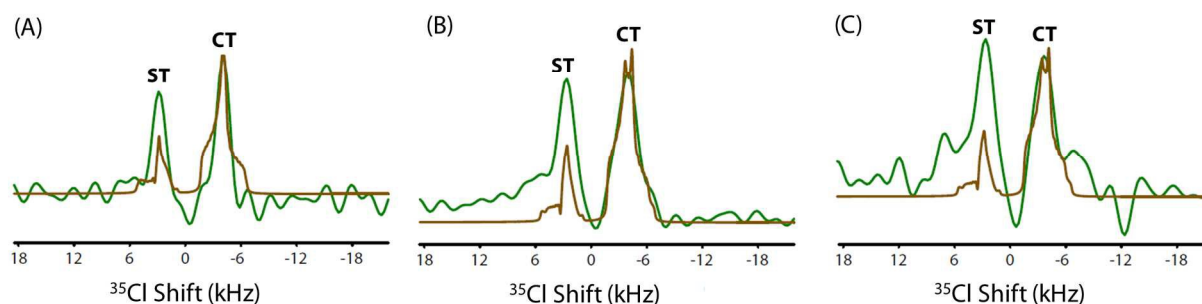
Figure 5. Simulated experimental lineshapes extracted parallel to the indirect frequency dimension at ^{1}H chemical shifts of 10 (A), 7.7 (B) and 4.5 (C) ppm of the proton-detected ^{35}Cl/^{1}H 2D D-HMQC correlation spectrum of L-Tyrosine.HCl obtained using a hard pulse irradiation of ^{35}Cl. The ^{35}Cl quadrupolar parameters (Qcc, η) obtained from lineshape fitting of three ^{35}Cl---^{1}H contacts at H2 (10 ppm), H1/H5/H9 (7.7 ppm) and H3 (4.5 ppm) resonances are

(2.2 MHz, 0.9), (2.3 MHz, 0.7) and (2.3 MHz, 0.7), respectively. All other simulation details are listed in **Figure 4** caption. The peak positions (isotropic second-order quadrupolar shift) of simulated lineshapes were adjusted to match the experimental shift (sum total of isotropic chemical shift and isotropic second-order quadrupolar shift).

To further cross validate the above findings we carried out the proton-detected $^{35}C/^{1}H$ 2D D-HMQC-based correlation experiment with a hard pulse irradiation of ^{35}Cl and rotor-synchronized acquisition on L-Histidine.HCl.H$_2$O (**Figure 6A**). The resulting $^{35}Cl/^{1}H$ 2D correlation spectrum with strong ST cross-peaks is shown in **Figure 6C**. Again, the ^{35}Cl shift observed from this experiment was verified from the 1D spectrum collected through the direct observation of ^{35}Cl using a single pulse experiment. One-dimensional ^{35}Cl experimental and simulated powder lineshapes of L-Histidine.HCl.H$_2$O are shown in **Figure 6B**. The calculated ^{35}Cl quadrupolar parameters for this sample from the 1D experiment are: Qcc = 1.8 MHz and η = 0.66 which agrees well with our previous observation with the same sample at 1020 MHz/ 24 T magnet (unpublished work).[32] From the 2D $^{35}Cl/^{1}H$ correlation spectrum shown in **Figure 6C**, six correlated (short and longer range) $^{35}Cl/^{1}H$ resonances are seen. The spectral slices taken parallel to the ^{35}Cl dimension at ^{1}H chemical shifts of NH^b, 1, NH$_3^+$, H$_2$O resonances of L-Histidine.HCl.H$_2$O were simulated to extract quadrupolar parameters. On the basis of the ST and CT peak separation and CT lineshape fitting (**Figure 6D**), the extracted quadrupolar parameters are listed in **Figure 6** caption. As seen in the case of L-Tyrosine.HCl, the ^{35}Cl quadrupolar parameters for L-Histidine.HCl.H$_2$O extracted at four ^{1}H chemical shifts are in close agreement with each other. However, these values are slightly different than that simulated from a directly observed 1D ^{35}Cl spectrum.
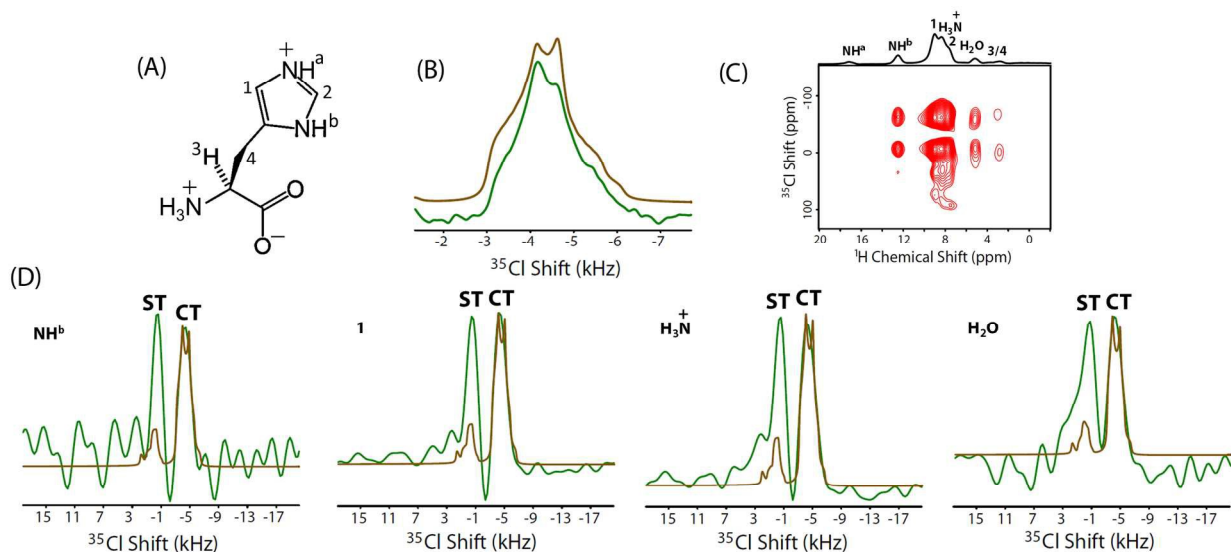
Figure 6. Molecular structure (A), the 1D ^{35}Cl experimental (green) spectrum collected using a hard pulse (1.35 μs) excitation, and 4291 scans and 5 s recycle delay (total experimental time = 5.96 hours) along with simulated lineshape (brown), a representative 2D ^{35}Cl/^{1}H D-HMQC spectrum measured using a hard pulse irradiation of ^{35}Cl (total experimental time = 63.7 hours) (C), simulated experimental lineshapes extracted parallel to the indirect frequency dimension at ^{1}H chemical shifts of NH^b, 1, NH$_3^+$, H$_2$O resonances of the proton-detected ^{35}Cl/^{1}H 2D D-HMQC correlation spectrum (D) of L-Histidine.HCl.H$_2$O. The ^{35}Cl quadrupolar parameters (Qcc, η) obtained from lineshape fitting of cross-peaks at NH^b, 1, NH$_3^+$ and H$_2$O ^{1}H resonances are (1.95 MHz, 0.45), (1.95 MHz, 0.45) , (1.95 MHz, 0.35), and (2.0 MHz, 0.45) respectively. All other simulation details are listed in **Figure 4** caption.

Once the applicability of the proton-detected ^{35}Cl/^{1}H 2D D-HMQC-based correlation measurement was established on L-Tyrosine.HCl and L-Histidine.HCl.H$_2$O, we carried out measurements on HCl salts of pharmaceutical ingredients, Amin and Proc (molecular structures are shown in **Figure S3** of the Supporting Information), to get insights into their structures in terms of chemical shift correlation (short and longer range) to protons and quadrupolar

16

parameters. One-dimensional ^{35}Cl spectra recorded at 600 MHz using a soft single pulse excitation under fast MAS (70 kHz) are demonstrated in **Figure 7 A** and **B** for Amin and Proc, respectively. The ^{35}Cl 1D spectrum of Amin results in a reasonably good powder lineshape that fits well with the numerical simulation. The extracted ^{35}Cl quadrupolar parameters for Amin, Qcc = 2.0 MHz and $\eta = 0.76$, are in a good agreement with the reported values.[1] Unlike Amin, a featureless ^{35}Cl 1D spectrum that suffers from huge distortions due to the probe ringing is observed for Proc which makes it impossible to extract any structural information. This observation should be attributed to the presence of a relatively large ^{35}Cl Qcc for this sample[1] that results in a poor sensitivity due to a quick decay of FID. Consequently, the ringing effect from the probe dominates the powder pattern. Similar phenomena was also observed by using 3.2 mm MAS probe at 600 MHz (data not shown). Next, we carried out the proton-detected ^{35}Cl/^{1}H 2D D-HMQC correlation measurement on these samples and ^{35}Cl/^{1}H cross-peaks observed in Amin and Proc are shown in **Figure 7C** and **D**, respectively. This observation is quite important especially for Proc in view of the fact that the ^{35}Cl 1D spectrum failed to offer any information about its structure. Furthermore, three different ^{35}Cl---^{1}H contacts are clearly observed from the ^{35}Cl/^{1}H 2D spectrum of Amin, a feature that is not possible to observe from the direct observation of ^{35}Cl. Similarly, one strong and few weak ^{35}Cl/^{1}H cross correlations observed in the case of Proc clearly highlights the importance of such measurement in order to understand the short and longer range ^{35}Cl---^{1}H contacts. Additionally, the exact ^{1}H resonances that correlate with ^{35}Cl can easily be assigned from the D-HMQC filtered 1D spectral slices shown in **Figure 8A** and **B** for Amin and Proc, respectively. More importantly, the improved resolution in the direct dimension unlike the 1D single pulse ^{1}H spectrum of Amin is the added benefit of carrying out such measurements for its structural studies. Low sensitivity of the D-

17

HMQC filtered 1D ^{1}H spectra (**Figure 8**) extracted from the 2D ^{35}Cl/^{1}H correlation spectra of Amin and Proc should be attributed to the presence of weak dipolar couplings between ^{1}H and ^{35}Cl, larger quadrupolar couplings, short ^{1}H T_2 and/or small amount of ^{35}Cl in these samples. Simulation of the spectral slice taken parallel to ^{35}Cl dimension at ^{1}H chemical shift of 10.4 ppm (**Figure S4** in the Supporting Information) for Proc resulted in quadrupolar parameters, Qcc = 4.45 MHz and $\eta = 0.52$. We would like to mention here that poor sensitivity of the experimental ^{35}Cl powder lineshape due to the presence of a huge quadrupolar coupling did not allow us to get the best fit from the numerical simulation. Instead, the quadrupolar parameters were approximately determined from the simulation on the basis of separation between the CT and ST peaks, and fitting the width of the CT peak. Besides, the quadrupolar parameters from the ^{35}Cl/^{1}H 2D measurement on Amin could not be determined again due to poor sensitivity of the ^{35}Cl powder lineshape. The requirement of a very long experimental time to accomplish ultimate sensitivity from the 2D correlation measurement due to a very long ^{1}H T_1 prevented us to try such experiments on Amin. It should be noted that the ^{35}Cl/^{1}H 2D correlation measurements have an additional benefit over the ^{35}Cl direct observation from the view point of the experimental setup. As mentioned above, based on ^{1}H T_1 relaxation time, the repetition time of ^{35}Cl/^{1}H measurement can be easily optimized. On the other hand, optimization of the repetition time of ^{35}Cl based on its T_1 relaxation time is mostly difficult to achieve from the direct observation method of ^{35}Cl. In other words, it is practically difficult to get optimized experimental conditions for the ^{35}Cl direct observation that should improve sensitivity unlike the proton detection-based approach for the indirect observation of ^{35}Cl presented in this study.
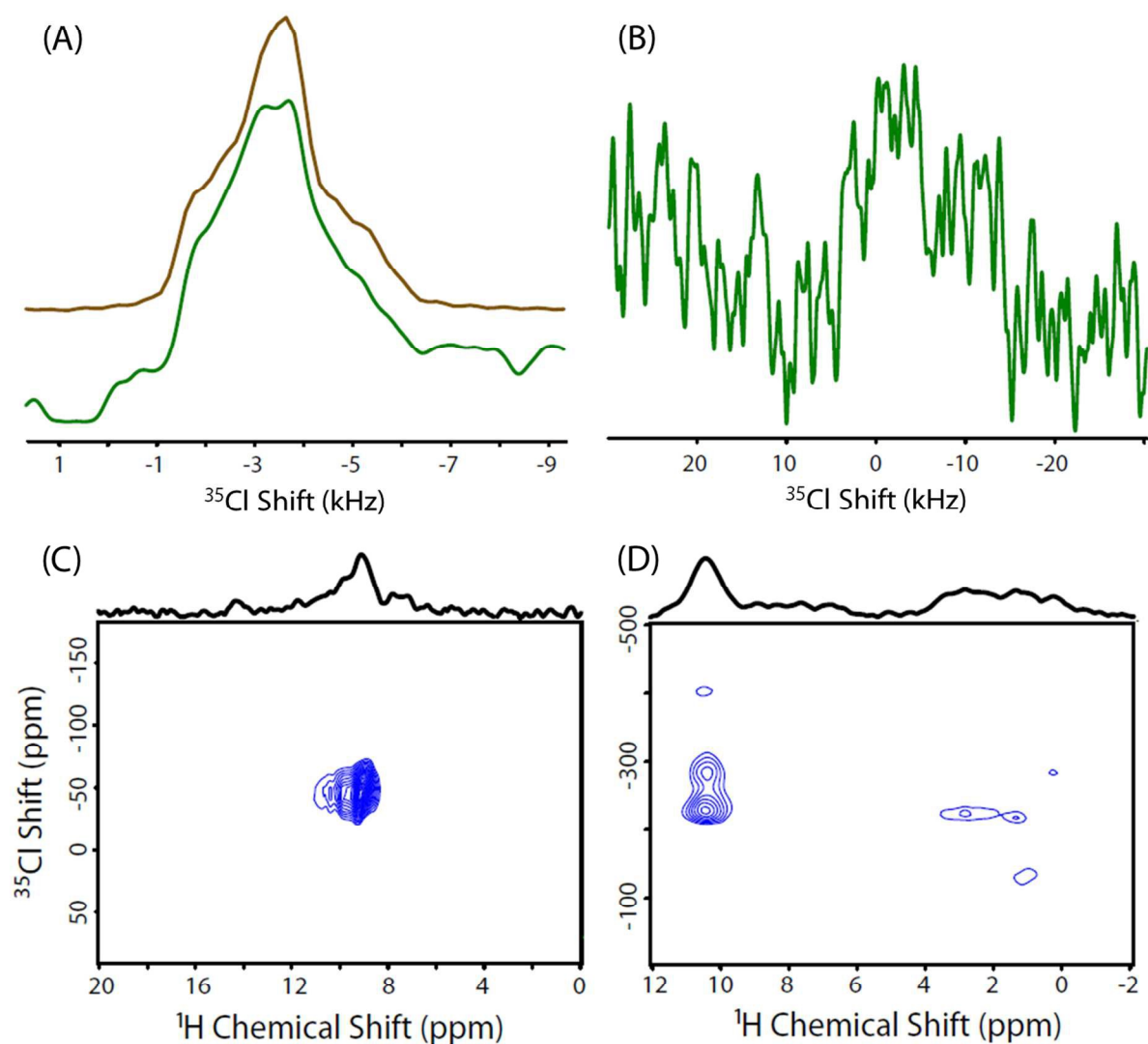
Figure 7. (A) One-dimensional ^{35}Cl experimental (green) using a soft pulse (13.5 μs) and simulated (brown) spectra of Amin (total experimental time = 1.7 hours (2993 scans and recycle delay = 2 s). (B) 1D ^{35}Cl experimental spectrum of Proc using a soft pulse of duration 8 μs (total experimental time = 0.47 hours (845 scans and recycle delay = 2 s)). (C) and (D) Representative 2D $^{35}Cl/^{1}H$ D-HMQC spectra of Amin (total experimental time = 34.1 hours) and Proc (total experimental time = 63.7 hours), respectively. Both 1D and 2D spectra were collected at 600 MHz spectrometer under 70 kHz MAS.
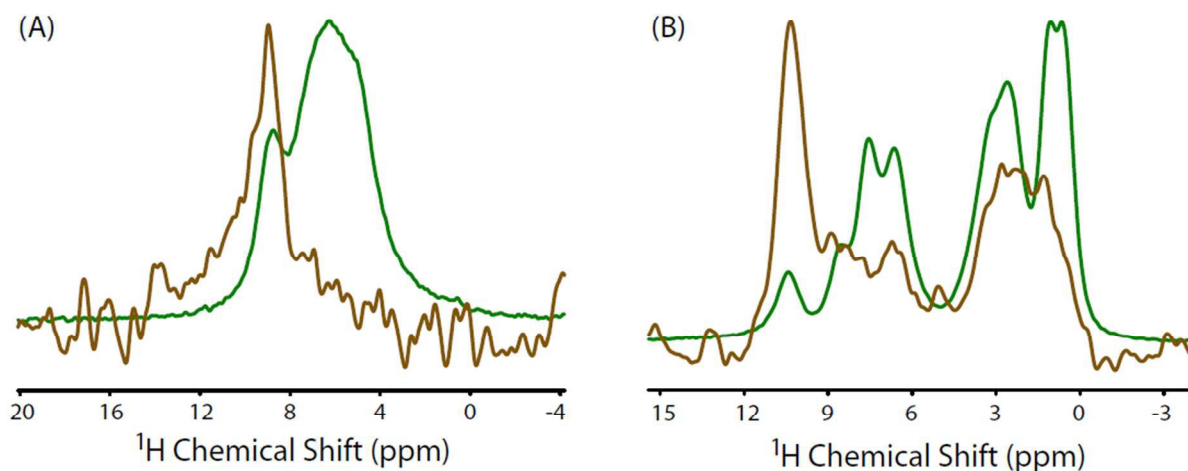
Figure 8. One-dimensional ^{1}H MAS spectra (green) collected using single pulse experiments under 70 kHz MAS at 600 MHz, and the 1D spectral slices (brown) taken parallel to the direct frequency dimension at ^{35}Cl shifts of -40.8 ppm and -227.0 ppm from the 2D D-HMQC spectra of Amin (A) and Proc (B), respectively.

Conclusion

In summary, we have demonstrated the applicability of proton detection-based approach to measure the 2D ^{35}Cl/^{1}H correlations in HCl salts of L-Tyrosine, LHistidine.HCl.H$_2$O and active pharmaceutical ingredients (APIs), Procainamide (Proc) and Aminoguanidine (Amin), utilizing a heteronuclear dipolar recoupling based D-HMQC experiment at fast MAS. The benefits of this approach, such as improved resolution and sensitivity, well-correlated ^{35}Cl/^{1}H peaks, and the absence of probe ringing issues over ^{35}Cl direct observation method, are highlighted. Moreover, we have demonstrated a method for a more accurate determination of quadrupolar parameters which is possible only if a hard pulse irradiation on ^{35}Cl is implemented in the 2D D-HMQC experiment. The quadrupolar parameters are obtained by simulating the lineshape inclusive of

CT and ST peaks. The separation between these peaks is shown to be extremely sensitive to both

Qcc and η. We believe that the present study will be a step forward in the structure

studies/refinement of systems with half integer quadrupolar nuclei.

References

(1)   Hildebrand, M.; Hamaed, H.; Namespetra, A. M.; Donohue, J. M.; Fu, R. Q.; Hung, I.; Gan, Z. H.; Schurko, R. W., Cl-35 Solid-State NMR of HCl Salts of Active Pharmaceutical Ingredients: Structural Prediction, Spectral Fingerprinting and Polymorph Recognition. *Cryst.Eng.comm* 2014, *16*, 7334-7356.

(2)   Singhal, D.; Curatolo, W., Drug Polymorphism and Dosage Form Design: A Practical Perspective. *Adv. Drug Deliver. Rev.* 2004, *56*, 335-347.

(3)   Reutzel-Edens, S. M., Achieving Polymorph Selectivity in the Crystallization of Pharmaceutical Solids: Basic Considerations and Recent Advances. *Curr. Opin. Drug Disc.* 2006, *9*, 806-815.

(4)   Hamaed, H.; Pawlowski, J. M.; Cooper, B. F. T.; Fu, R. Q.; Eichhorn, S. H.; Schurko, R. W., Application of Solid-State ^{35}Cl NMR to the Structural Characterization of Hydrochloride Pharmaceuticals and Their Polymorphs. *J. Am. Chem. Soc.* 2008, *130*, 11056-11065.

(5)   Brittain, H. G.; Grant, D. J. W., Effect of Polymorphism and Solid-State Solvation on Solubility and Dissolution Rate. *In H.G. Brittain (ed.) Polymormphism in Pharmaceutical Solids, Marcel Dekker, Inc., New York* 1999, 279-330.

(6)   Zell, M. T.; Padden, B. E.; Grant, D. J. W.; Schroeder, S. A.; Wachholder, K. L.; Prakash, I.; Munson, E. J., Investigation of Polymorphism in Aspartame and Neotame Using Solid-State NMR Spectroscopy. *Tetrahedron* 2000, *56*, 6603-6616.

(7)   Padden, B. E.; Zell, M. T.; Dong, Z. D.; Schroeder, S. A.; Grant, D. J. W.; Munson, E. J., Comparison of Solid-State ^{13}C NMR Spectroscopy and Powder X-Ray Diffraction for Analyzing Mixtures of Polymorphs of Neotame. *Anal. Chem.* 1999, *71*, 3325-3331.

(8)   Chapman, R. P.; Widdifield, C. M.; Bryce, D. L., Solid-State NMR of Quadrupolar Halogen Nuclei. *Prog. Nucl. Magn. Reson. Spectro.* 2009, *55*, 215-237.

(9)   Widdifield, C. M.; Chapman, R. P.; Bryce, D. L., Chlorine, Bromine, and Iodine Solid-State NMR Spectroscopy. *Annu Rep NMR Spectro.* 2009, *66*, 195-326.

(10)   Samoson, A.; Lippmaa, E.; Pines, A., High-Resolution Solid-State NMR Averaging of 2nd-Order Effects by Means of a Double-Rotor. *Mol. Phys.* 1988, *65*, 1013-1018.

(11)   Wooten, E. W.; Mueller, K. T.; Pines, A., New Angles in Nuclear-Magnetic-Resonance Sample Spinning. *Acc. Chem. Res.* 1992, *25*, 209-215.

(12)   Mueller, K. T.; Sun, B. Q.; Chingas, G. C.; Zwanziger, J. W.; Terao, T.; Pines, A., Dynamic-Angle Spinning of Quadrupolar Nuclei. *J. Magn. Reson.* 1990, *86*, 470-487.

(13)   Medek, A.; Harwood, J. S.; Frydman, L., Multiple-Quantum Magic-Angle Spinning Nmr: A New Method for the Study of Quadrupolar Nuclei in Solids. *J. Am. Chem. Soc.* 1995, *117*, 12779-12787.

(14)   Agarwal, V.; Penzel, S.; Szekely, K.; Cadalbert, R.; Testori, E.; Oss, A.; Past, J.; Samoson, A.; Ernst, M.; Bockmann, A.; Meier, B. H., De Novo 3D Structure Determination from Sub-Milligram Protein Samples by Solid-State 100 KHz MAS NMR Spectroscopy. *Angew. Chem.* 2014, *53*, 12253-12256.

(15)   Kobayashi, T.; Mao, K.; Paluch, P.; Nowak-Krol, A.; Sniechowska, J.; Nishiyama, Y.; Gryko, D. T.; Potrzebowski, M. J.; Pruski, M., Study of Intermolecular Interactions in the Corrole Matrix by Solid-State Nmr under 100 KHz MAS and Theoretical Calculations. *Angew. Chem. Int. Ed.* 2013, *52*, 14108-14111.

(16)   Nishiyama, Y.; Lu, X.; Trebosc, J.; Lafon, O.; Gan, Z.; Madhu, P. K.; Amoureux, J. P., Practical Choice of ^{1}H-^{1}H Decoupling Schemes in through-Bond ^{1}H-{X} HMQC Experiments at Ultra-Fast MAS. *J. Magn. Reson.* 2012, *214*, 151-158.

(17)   Cavadini, S.; Antonijevic, S.; Lupulescu, A.; Bodenhausen, G., Indirect Detection of Nitrogen-14 in Solids Via Protons by Nuclear Magnetic Resonance Spectroscopy. *J. Magn. Reson.* 2006, *182*, 168-172.

(18)   Cavadini, S.; Lupulescu, A.; Antonijevic, S.; Bodenhausen, G., Nitrogen-14 NMR Spectroscopy Using Residual Dipolar Splittings in Solids. *J. Am. Chem. Soc.* 2006, *128*, 7706-7707.

(19)   Cavadini, S., Indirect Detection of Nitrogen-14 in Solid-State NMR Spectroscopy. *Prog. Nucl. Magn. Reson. Spectro.* 2010, *56*, 46-77.

(20)   Gan, Z. H., Measuring Amide Nitrogen Quadrupolar Coupling by High-Resolution ^{14}N/^{13}C NMR Correlation under Magic-Angle Spinning. *J. Am. Chem. Soc.* 2006, *128*, 6040-6041.

(21)   Pandey, M. K.; Nishiyama, Y., Proton-Detected 3D ^{14}N/^{14}N/^{1}H Isotropic Shift Correlation Experiment Mediated through ^{1}H-^{1}H RFDR Mixing on a Natural Abundant Sample under Ultrafast MAS. *J. Magn. Reson.* 2015, *258*, 96-101.

(22)   Nishiyama, Y.; Endo, Y.; Nemoto, T.; Utsumi, H.; Yamauchi, K.; Hioka, K.; Asakura, T., Very Fast Magic Angle Spinning ^{1}H-^{14}N 2D Solid-State NMR: Sub-Micro-Liter Sample Data Collection in a Few Minutes. *J. Magn. Reson.* 2011, *208*, 44-48.

(23)   Gan, Z. H.; Amoureux, J. P.; Trebosc, J., Proton-Detected ^{14}N MAS NMR Using Homonuclear Decoupled Rotary Resonance. *Chem. Phys. Lett.* 2007, *435*, 163-169.

(24)   Trebosc, J.; Hu, B.; Amoureux, J. P.; Gan, Z., Through-Space R^3-HETCOR Experiments between Spin-1/2 and Half-Integer Quadrupolar Nuclei in Solid-State NMR. *J. Magn. Reson.* 2007, *186*, 220-227.

(25)   Bryce, D. L.; Sward, G. D.; Adiga, S., Solid-State $^{35/37}$Cl NMR Spectroscopy of Hydrochloride Salts of Amino Acids Implicated in Chloride Ion Transport Channel Selectivity: Opportunities at 900 MHz. *J. Am. Chem. Soc.* 2006, *128*, 2121-2134.

(26)   Mafra, L.; Siegel, R.; Fernandez, C.; Schneider, D.; Aussenac, F.; Rocha, J., High-Resolution ^{1}H Homonuclear Dipolar Recoupling NMR Spectra of Biological Solids at MAS Rates up to 67 KHz. *J. Magn. Reson.* 2009, *199*, 111-114.

(27)   Frey, M. N.; Koetzle, T. F.; Lehmann, M. S.; Hamilton, W. C., Precision Neutron-Diffraction Structure Determination of Protein and Nucleic-Acid Components .X. Comparison between Crystal and Molecular-Structures of L-Tyrosine and L-Tyrosine Hydrochloride. *J. Chem. Phys.* 1973, *58*, 2547-2556.

(28)   Maruyoshi, K.; Iuga, D.; Antzutkin, O. N.; Alhalaweh, A.; Velagad, S. P.; Brown, S. P., Identifying the Intermolecular Hydrogen-Bonding Supramolecular Synthons in an

Indomethacin-Nicotinamide Cocrystal by Solid-State NMR. *Chem. Comm.* 2012, *48*, 10844-10846.

(29)   Tatton, A. S.; Pham, T. N.; Vogt, F. G.; Iuga, D.; Edwards, A. J.; Brown, S. P., Probing Intermolecular Interactions and Nitrogen Protonation in Pharmaceuticals by Novel N-15-Edited and 2D ^{14}N-^{1}H Solid-State NMR. *Cryst.Eng.Comm.* 2012, *14*, 2654-2659.

(30)   Tatton, A. S.; Pham, T. N.; Vogt, F. G.; Iuga, D.; Edwards, A. J.; Brown, S. P., Probing Hydrogen Bonding in Cocrystals and Amorphous Dispersions Using ^{14}N-^{1}H HMQC Solid-State NMR. *Mol. Pharm.*2013, *10*, 999-1007.

(31)   Cavadini, S.; Antonijevic, S.; Lupulescu, A.; Bodenhausen, G., Indirect Detection of Nitrogen-14 in Solid-State NMR Spectroscopy. *Chem.Phys.Chem* 2007, *8*, 1363-1374.

(32)   Pandey, M. K., et al., 1.02 Ghz/24 T High Resolution and Sensitivity Solid-State NMR Measurements of Low-Gamma Half-Integer Quadrupolar Nuclei ^{35}Cl and ^{37}Cl. *Submitted* 2015.